

In Silico Assessment of Tanning Masking Effects on Skin Chromatic Attributes Elicited by Anemia and Hyperbilirubinemia

Gladimir V. G. Baranoski¹ and Petri M. Varsa¹

Abstract—Changes in skin appearance are among the most recognizable symptoms of a number of medical conditions. The interpretation of such changes, however, may be inadvertently biased by normal physiological processes affecting skin optical properties. In this paper, we assess the impact of one of the most common of these processes, tanning, on variations in skin chromatic attributes elicited by two ubiquitous and serious medical conditions, anemia and hyperbilirubinemia. We employ a first-principles investigation approach centered on the use of predictive computer simulations of light and skin interactions, and on well-established colorimetry methods. In our *in silico* experiments, we considered skin chromatic attributes resulting from distinct anemia severity levels and hyperbilirubinemia toxicity stages. Our findings highlight qualitative and quantitative aspects that need to be considered in the visual screening and monitoring of these conditions, notably when they occur with the concomitant presence of tanning-induced changes in the cutaneous tissues' melanin pigmentation and thickness.

Index Terms—skin, reflectance, color perception, tanning, anemia, hyperbilirubinemia, screening, monitoring, simulation.

I. INTRODUCTION

Anemia and hyperbilirubinemia are pervasive medical conditions, affecting the health of individuals of all ages, genders and ethnicities worldwide [1], [2]. Although both conditions can be successfully addressed in most cases, their early detection is essential to mitigate more serious consequences. The efficacy of any initiative in this area relies on the understanding about their triggering factors and elicited symptoms. Among these symptoms, one can include changes in skin appearance, particularly in its chromatic attributes, the focal point of this investigation.

Anemia can be concisely described as a disorder associated with a decrease in the number of red blood cells encapsulating hemoglobin [3], [4]. The two functional forms of this protein, namely oxyhemoglobin and deoxyhemoglobin, corresponds to the oxygenated and deoxygenated states of its molecules. While the former contains iron atoms in a ferrous state that allows them to bind with oxygen, the latter contains iron atoms in a ferric (oxidized) state that prevents this binding. Accordingly, a reduction in the supply of these proteins can seriously hinder the blood's capability of transporting oxygen from respiratory organs to the rest of the body [5], which can lead to life-threatening situations [1], [3].

*This work was supported in part by the Natural Sciences and Research Council of Canada (NSERC) under Grant 238337.

¹ Gladimir V. G. Baranoski and Petri Varsa are with the Natural Phenomena Simulation Group, School of Computer Science, University of Waterloo, 200 University Avenue, Waterloo, Ontario, N2L 3G1, Canada. gvgbaran@cs.uwaterloo.ca

When aging red blood cells are removed from blood circulation, the breakdown of hemoglobin results in byproducts, notably bilirubin [2]. Under normal physiological conditions, bilirubin is removed from the blood stream by the liver. In simple terms, hyperbilirubinemia corresponds to an abnormal presence of bilirubin in an individual's blood stream [6]. The most serious form of this disorder occurs when the hemoglobin breakdown is accelerated and/or hepatic activity is reduced [7]. Different types of encephalopathy, including irreversible brain damage, [8], [9], and pigment gallstones [2], [7] are among its most detrimental consequences.

Since both conditions are connected with changes in the blood composition, they are compelled to affect skin optical properties, principally in the dermal layers characterized by the presence of blood vessels. More specifically, a reduction of hemoglobin concentration associated with the onset of anemia can result in a pale skin appearance [3], [4]. In the case of hyperbilirubinemia, a yellow-tinted skin appearance (commonly referred to as jaundice) [10], [11] is elicited by an increase in the concentration of bilirubin, which can also be found outside dermal blood vessels and in the epidermal layers [6]. Although these skin chromatic variations associated with anemia and hyperbilirubinemia are usually specifically tied to the absorption spectra of hemoglobin (Fig. 1(a)) and bilirubin (Fig. 1(b)), respectively, they may also result from their combined effects on light attenuation within the cutaneous tissues since an individual can be subjected to both conditions at the same time [12], [13], [14], [15], [16].

These variations in skin chromatic attributes, however, can be considerably masked by an individual's melanin pigmentation level. This can be attributed to the fact that both forms of this pigment, eumelanin and pheomelanin, found within the epidermal layers are characterized by strong light absorption capabilities in the visible spectral domain (Fig. 1(c)). To date, most investigations on these masking effects have been focused on different levels of constitutive pigmentation (resulting from genetic factors) [4], [17], [18].

To the extent of our knowledge, investigations on the masking effects resulting from distinct levels of facultative pigmentation (elicited by environmental factors such as exposure to ultraviolet radiation (UVR)), particularly considering the simultaneous onset of anemia and hyperbilirubinemia, have not as yet been reported in the literature. This research gap may be attributed to the intrinsic limitations of traditional laboratory procedures. For instance, a systematic reduction in hemoglobin concentration and increase in bilirubin concentration may be problematic to be achieved/controlled. Moreover, it could also pose risks to a subject's health, which

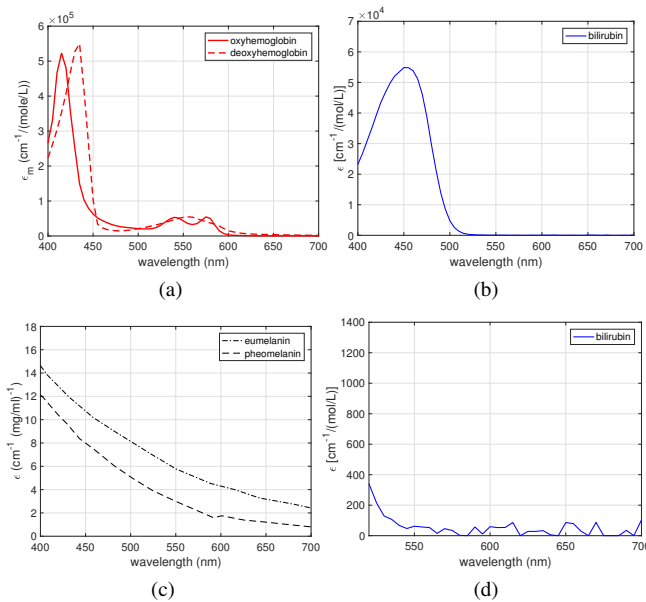


Fig. 1: Absorption spectra of key pigments considered in this investigation. (a) Functional hemoglobins' molar extinction coefficient [22]. (b) Bilirubin molar extinction coefficient [23], [24]. (c) Melanins' extinction coefficient [25]. (d) Zoom-in plot of the curve depicted in (b).

could be further affected by overexposure to UVR.

Through the investigation presented in this paper, we intend to contribute to the mitigation of this gap. More explicitly, we examine the effects of UVR-triggered delayed tanning [19], henceforth referred simply as tanning, on the skin chromatic attributes elicited by anemia and hyperbilirubinemia, occurring separately or simultaneously. These effects, in turn, are associated not only with melanogenesis-induced changes in melanin content and distribution within the cutaneous tissues, but also with hyperplasia-induced changes in their morphology (thickness) [20].

To overcome the aforementioned laboratory constraints, we employed a computational (*in silico* [21]) experimental framework supported by measured data provided in the related biomedical literature. The analysis of skin chromatic variations obtained through our *in silico* experiments, which was performed using empirical perceptibility thresholds reported in the related colorimetry literature, has revealed trends that need to be accounted for in the development of effective protocols for the visual screening and monitoring of these medical conditions.

II. MATERIALS AND METHODS

In our investigation, we considered a typical skin specimen with a moderate tanning ability. The parameter values employed in its characterization are provided in Tables I and II. For its untanned state, the selection of parameter values was based on biophysically valid ranges whose literature sources are listed elsewhere [26], [27] for conciseness. For its tanned state, we employed parameter values obtained considering the peak of a tanning process, which was carefully reproduced using a physiologically-based platform for the

TABLE I: Parameters employed in characterization of the selected specimen in its untanned (U) and tanned (T) states.

Parameter	Value (U)	Value (T)
SC Thickness (<i>cm</i>)	0.001	0.00116
SG Thickness (<i>cm</i>)	0.0011	0.00128
SS Thickness (<i>cm</i>)	0.0011	0.00128
SB Thickness (<i>cm</i>)	0.0011	0.00128
PD Thickness (<i>cm</i>)	0.04	0.0465
RD Thickness (<i>cm</i>)	0.1	0.1162
SG Melanosome Content (%)	0.21	1.45
SS Melanosome Content (%)	0.43	0.72
SB Melanosome Content (%)	0.80	0.50
SG Colloidal Melanin Content (%)	1.03	7.09
SS Colloidal Melanin Content (%)	2.9	3.50
SB Colloidal Melanin Content (%)	3.9	2.46

Note: The acronyms SC, SG, SS, SB, PD and RD refer to the stratum corneum, stratum granulosum, stratum spinosum, stratum basale, papillary dermis and reticular dermis tissues, respectively.

simulation of skin tanning dynamics [19] driven by actual photobiological experiments. More precisely, we accounted for an $\approx 86\%$ increase in the total melanin content (nonuniformly distributed within the epidermal layers) and an $\approx 16\%$ increase in the cutaneous tissues' thickness. For brevity, the reader interested in more details about the computation of these values is referred to the related cited works [19], [20].

It has been noted that, although the hemoglobin concentration in the blood alone cannot be used to diagnose anemia, it can provide useful information for determining its severity level [1], [4]. Thus, in our investigation, we considered anemia severity levels associated with distinct intravascular hemoglobin concentrations within the dermal tissues. The values assigned to these concentrations, which are present in Table III, were also selected according to ranges specified in the literature [1], [4], [28], [29].

Regarding the hyperbilirubinemia component of our investigation, we considered intravascular bilirubin concentrations derived from total serum bilirubin (TSB) values reported in the literature for baseline (normal), significant (associated with noticeable signs of bilirubin toxicity), excessive (associated with potentially irreversible bilirubin-induced physiological damages) and extreme (associated with high risks of mortality) levels of bilirubin present in the blood stream [7], [8], [30]. These TSB values were then multiplied by 0.55 to obtain the intravascular bilirubin concentrations, which are presented in Table IV, associated with distinct hyperbilirubinemia toxicity states. This scaling step was performed since plasma, the bilirubin transporting medium, normally accounts for 55% of the blood volume [31]. The extravascular contents of bilirubin within the cutaneous tissues were estimated by multiplying the values listed in Table IV by a standard bilirubin transference factor equal to 0.2 [6].

To perform our *in silico* experiments, we initially employed a first-principles model of light and skin interactions, known as HyLIoS (*Hyperspectral Light Impingement on Skin*) [26]. More precisely, we used it to compute the directional-hemispherical reflectance curves associated with the selected specimen in its untanned and tanned states, and subject to distinct anemia severity levels and hyperbilirubinemia toxicity stages. Within HyLIoS' ray-optics

TABLE II: Parameters kept fixed during the simulations.

Parameter	Value
Ratio of Skin Surface Folds	0.1
Melanosome Dimensions ($\mu m \times \mu m$)	0.41×0.17
Melanosome Eumelanin Concentration (g/L)	50.0
Melanosome Pheomelanin Concentration (g/L)	2.0
Melanin Refractive Index	1.7
Blood Content (%)	0.2
RD Blood Content (%)	0.2
Dermal Oxyhemoglobin Fraction (%)	90.0
Methemoglobin Concentration in Blood (g/L)	1.5
Carboxyhemoglobin Concentration in Blood (g/L)	1.5
Sulfhemoglobin Concentration in Blood (g/L)	0.0
Beta-Carotene Concentration (g/L)	2.1E-4
Epidermis Beta-Carotene Concentration (g/L)	2.1E-4
Blood Beta-Carotene Concentration (g/L)	7.0E-5
SC Water Content (%)	35.0
Epidermis Water Content (%)	60.0
PD Water Content (%)	75.0
RD Water Content (%)	75.0
SC Lipid Content (%)	20.0
Epidermis Lipid Content (%)	15.1
PD Lipid Content (%)	17.33
RD Lipid Content (%)	17.33
SC Keratin Content (%)	65.0
SC Urocanic Acid Density (mol/L)	0.01
Skin DNA Density (g/L)	0.185
Melanin Refractive Index	1.7
SC Refractive Index	1.55
Epidermis Refractive Index	1.4
PD Refractive Index	1.39
RD Refractive Index	1.41
PD Scatterers Refractive Index	1.5
Radius of PD Scatterers (nm)	70.0
PD Fraction Occupied by Scatterers (%)	22.0

Note: The acronyms SC, SG, SS, SB, PD and RD refer to the stratum corneum, stratum granulosum, stratum spinosum, stratum basale, papillary dermis and reticular dermis tissues, respectively.

algorithmic formulation, a ray interacting with the tissues of a skin specimen can be associated with any wavelength (λ) within a spectral region of interest. It is worth noting that HyLIoS' predictive capabilities have been extensively evaluated through quantitative and qualitative comparisons of its outcomes with actual measured data [26]. Since then, this model has been effectively employed in several related biomedical investigations (e.g., [4], [19], [27], [32], [33]).

For consistency, we adopted a spectral resolution of 5 nm in all reflectance curves presented in this work, which were obtained using a virtual spectrophotometer [34]. In their computation, we considered an angle of incidence of 15° and employed 10^6 sample rays (per λ). To enable the reproduction of our findings and the future extensions of our investigation by the biomedical community, we made HyLIoS available online [35], [36] along with the supporting biophysical datasets (e.g., refractive index and extinction coefficient curves [37]) used in this work.

Subsequently, we employed the modeled reflectance curves to generate the skin chromatic attributes resulting from the physiological changes under investigation. More specifically, these attributes were computed through the convolution of a selected illuminant's relative spectral power distribution, the modeled reflectance data and the broad spectral response of the human photoreceptors [38]. This last step was performed by employing a standard CIEXYZ to sRGB color

TABLE III: Anemia severity levels.

Level	Severity	Hemoglobin Concentration (g/L)
A0	baseline	147.0
A1	mild	117.6
A2	moderate	88.2
A3	severe	58.8

Note: the reductions in hemoglobin concentration were selected according to ranges specified in the literature [1], [4], [28], [29].

TABLE IV: Hyperbilirubinemia toxicity stages.

Stage	Toxicity	Bilirubin Concentration (g/L)
H0	baseline	0.003
H1	significant	0.071
H2	excessive	0.161
H3	extreme	0.233

Note: the increases in bilirubin concentration were selected according to values provided in the literature [6], [7], [8], [30].

system conversion procedure [39] and considering the CIE D50 illuminant [38]. The resulting colors were then used to generate skin swatches through the application of a grayscale texture.

Besides the visual inspection of the skin swatches, we also used a device-independent CIE-based metric to compare the modeled skin chromatic attributes. More precisely, we calculated the CIELAB differences between the colors (before their achromatic relative brightness modulation by the grayscale texture) associated with pairs of swatches using the following formula [40]:

$$\Delta E_{ab}^* = \sqrt{(d_L^2 + d_a^2 + d_b^2)}, \quad (1)$$

where d_L , d_a and d_b represent the differences $L_1^* - L_2^*$, $a_1^* - a_2^*$ and $b_1^* - b_2^*$, respectively, in which L^* , a^* and b^* correspond the CIELAB color space dimensions. These are calculated for the modeled chromatic attributes (colors) associated with the compared swatches (indicated by the subscripts 1 and 2, respectively). Again, we performed these calculations using standard formulas employed in colorimetry [41] and considering the CIE D50 illuminant [38].

III. RESULTS AND DISCUSSION

We started our *in silico* experiments by computing the reflectance curves for the selected specimen in its untanned state. As it can be observed in the graphs presented in Fig. 2(a), an increase in the anemia severity level is accompanied by an overall increase in the reflectance curves when one considers a normal amount of bilirubin present in the specimen's tissues. Moreover, as expected [4], this increase is more noticeable between 500 and 600 nm, which corresponds to a spectral region in which light absorption by the hemoglobins is significant (Fig. 1(a)) and less affected by the melanins' absorption spectra (Fig. 1(c)).

However, as depicted in the graphs presented in Figs. 2(b) to (d), the reflectance increase elicited by anemia is not observed between 400 and 475 nm when one considers the hyperbilirubinemia toxicity stages H1 to H3. In fact, one can notice a slight decrease in the reflectance curves in this

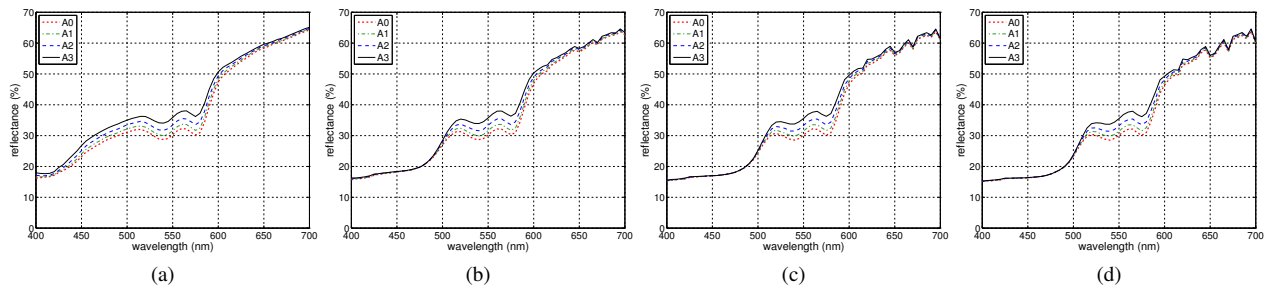


Fig. 2: Graphs depicting changes in the reflectance curves obtained for the selected specimen in its untanned state. Changes resulted from variations in anemia severity levels (Table III), from A0 (baseline), A1 (mild), A2 (moderate) to A3 (severe), and in hyperbilirubinemia toxicity stages (Table IV). From (a) to (d), the graphs were obtained considering the hyperbilirubinemia toxicity stages H0 (baseline), H1 (significant), H2 (excessive) and H3 (extreme), respectively.

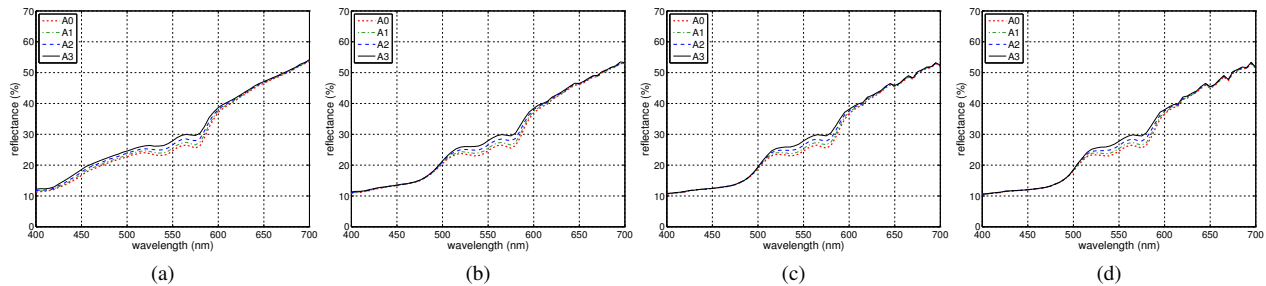


Fig. 3: Graphs depicting changes in the reflectance curves obtained for the selected specimen in its tanned state. Changes resulted from variations in anemia severity levels (Table III), from A0 (baseline), A1 (mild), A2 (moderate) to A3 (severe), and in hyperbilirubinemia toxicity stages (Table IV). From (a) to (d), the graphs were obtained considering the hyperbilirubinemia toxicity stages H0 (baseline), H1 (significant), H2 (excessive) and H3 (extreme), respectively.

spectral region, which can be attributed to the absorption spectrum of bilirubin (Fig. 1(b)). In addition, the differences between the reflectance values computed for the distinct anemia severity stages become negligible.

Furthermore, one can also notice reflectance variations between 620 and 700 nm, which can be associated to “peaks” in the absorption spectrum of bilirubin in this region (Fig. 1(d)). As expected [6], these variations become more noticeable as the amount of bilirubin in the specimen’s tissues increases.

We then generated the skin swatches associated with the reflectance curves presented in Fig. 2. These swatches, which are presented in Fig. 4, show the corresponding changes in the skin chromatic attributes of the selected specimen in its untanned state and subjected to distinct anemia severity levels and hyperbilirubinemia toxicity stages. When one considers just the increase in the anemia severity level (Fig. 4 (top row)), one can observe a characteristic change to a pale hue. On the other hand, considering just the increase in hyperbilirubinemia toxicity stage (Fig. 4 (left column)), one can observe a strong change to a yellowish hue. When both are increased, the resulting chromatic variations become less gradual, to the point that becomes difficult to visually distinguish one swatch color from another.

In order to quantify these color variations, we employed the CIELAB ΔE_{ab}^* differences. It has been experimentally determined that the perceptibility threshold for these differences is 2.3 [40], [42], *i.e.*, chromatic variations associ-

ated with ΔE_{ab}^* below 2.3 are not considered discernible by human observers in general. The row-wise differences computed for the swatches depicted in Fig. 4 are presented in Table V, and they were below this threshold only in four cases (out of 12) associated with color variations linked to transitions involving the lowest anemia severity levels (from A0 to A1). The column-wise differences computed for these swatches are presented in Table VI, and they were below 2.3 only in four cases as well, albeit associated with color variations linked to transitions involving the highest hyperbilirubinemia toxicity stages (from H2 and H3).

In the next round of our *in silico* experiments, in which we considered the selected specimen in its tanned state, we again started by computing its reflectance curves considering the distinct anemia severity levels and hyperbilirubinemia toxicity stages. As it can be verified in the graphs presented in Fig. 3, these curves depict the same qualitative trends observed considering the specimen in its untanned state (Fig. 2). However, one can notice distinct quantitative traits. More exactly, the curves obtained for the specimen in its tanned state are overall lower than those obtained for the specimen in its untanned state. Moreover, the curves associated with distinct anemia severity levels are close to each other, and the changes in the 620 to 700 nm region, which were elicited by an increase presence of bilirubin in specimen’s tissues, are less pronounced. These quantitative aspects can be attributed to the increase in the specimen’s facultative pigmentation, which led to an overall increase in

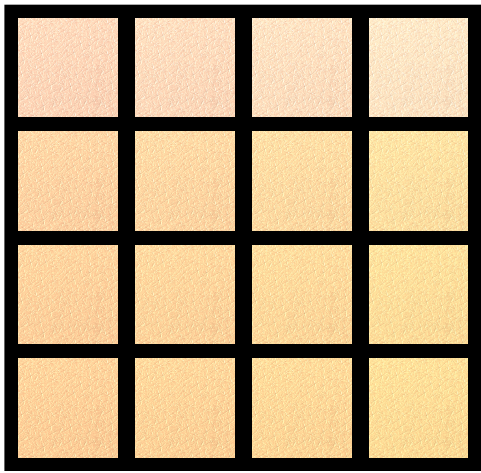


Fig. 4: Skin swatches obtained using the reflectance curves provided in Fig. 2 for the selected specimen in its untanned state. From left to right, the swatches in each column correspond to anemia severity levels A0 (baseline), A1 (mild), A2 (moderate) and A3 (severe), respectively. From top to bottom, the swatches in each row correspond to hyperbilirubinemia toxicity stages H0 (baseline), H1 (significant), H2 (excessive) and H3 (extreme), respectively.

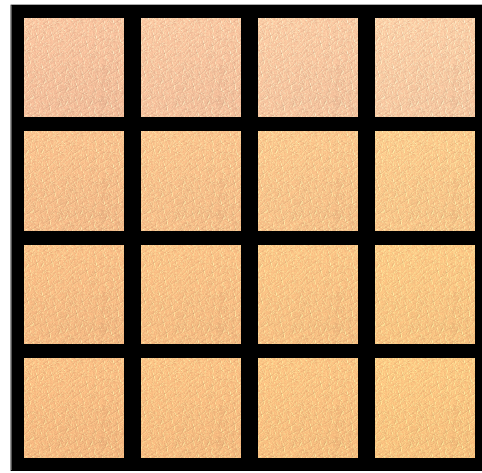


Fig. 5: Skin swatches obtained using the reflectance curves provided in Fig. 3 for the selected specimen in its tanned state. From left to right, the swatches in each column correspond to anemia severity levels A0 (baseline), A1 (mild), A2 (moderate) and A3 (severe), respectively. From top to bottom, the swatches in each row correspond to hyperbilirubinemia toxicity stages H0 (baseline), H1 (significant), H2 (excessive) and H3 (extreme), respectively.

the amount of light absorbed by the melanins, the dominant visible light absorbers found in human skin [39].

Similar to the previous round of experiments, we proceeded to generate the swatches associated with the reflectance curves presented in Fig. 3. These swatches, presented in Fig. 5, show the corresponding changes in the skin chromatic attributes of the selected specimen in its tanned state and subjected to distinct anemia severity levels and hyperbilirubinemia toxicity stages. An initial visual inspection of these swatches revealed the same qualitative trends observed in the swatches presented in Fig. 4. More precisely, one can also observe changes to pale and yellowish hues when one considers just the separate effects of anemia and hyperbilirubinemia, respectively. However, the resulting swatches' paleness and yellowness were less noticeable than those observed for the specimen in its untanned state.

To assess the impact of tanning on the color variations between the swatches depicted in Fig. 5, we employed the CIELAB ΔE_{ab}^* differences once more. The obtained ΔE_{ab}^* values unveiled a markedly distinct quantitative trend regarding the color variations elicited by anemia and hyperbilirubinemia. The row-wise differences computed for the swatches associated with the former are presented in Table VII. In contrast with the values obtained for the specimen in its untanned state, the ΔE_{ab}^* values were below the 2.3 threshold in 11 (out of 12) cases. The column-wise differences computed for the swatches associated with the latter are presented in Table VIII. Like the values obtained for the specimen in its untanned state, they were below 2.3 only in four cases associated with color variations linked to transitions involving the highest hyperbilirubinemia toxicity stages (from H2 and H3).

In recent years, many approaches have been proposed to address the medical needs of populations living in areas with limited access to physicians and specialized diagnostic equipment. These approaches often involve the use of relatively low cost cameras to facilitate the initial screening and monitoring of medical conditions affecting those populations. However, several technical aspects, such as the spectral light distribution of the light sources and illumination/viewing conditions, just to name a few, need to be controlled to ensure an appropriate degree of fidelity and consistency in the acquisition of digital data. Furthermore, it is necessary to take into account possible changes in a patient's physiological and health status between the collection of photographic records. Although the connections of such changes with the target condition and its symptoms may not be readily detectable, they may hinder the correct interpretation of those records.

Tanning is arguably among the most common physiological changes affecting human appearance. The skin swatches presented in Figs. 4 and 5 indicate that tanning-induced changes in cutaneous tissues' melanin pigmentation and thickness can alter the degree of paleness and yellowness that one would expect to follow the onset of anemia and hyperbilirubinemia, respectively. Furthermore, our findings, particularly those related to the CIELAB chromatic differences associated with the swatches generated for the specimen in its tanned state, indicate a higher degree of difficulty in the differentiation of variations in skin color attributes associated with the onset of anemia (Table VII) than those brought about by hyperbilirubinemia (Table VIII).

Hence, when using visual records to support the screening of distinct anemia severity levels and hyperbilirubinemia toxicity stages during a given time period, one should pay

TABLE V: Row-wise CIELAB ΔE_{ab}^* values computed for the (untanned) specimen’s swatches depicted in Fig 4.

Hyperbilirubinemia Toxicity Stages	Anemia Severity Transitions		
	A0 & A1	A1 & A2	A2 & A3
H0	1.4941	2.4602	2.9653
H1	1.8897	3.4710	3.1428
H2	1.8841	2.8347	4.0730
H3	1.8811	2.8282	4.0646

Note: Values below the perceptibility threshold (2.3) for CIELAB chromatic differences are presented in boldface.

TABLE VI: Column-wise CIELAB ΔE_{ab}^* values computed for the (untanned) specimen’s swatches depicted in Fig 4.

Hyperbilirubinemia Toxicity Transitions	Anemia Severity Levels			
	A0	A1	A2	A3
H0 & H1	9.2849	10.2381	12.6477	14.2340
H1 & H2	2.4813	2.4693	2.3954	2.8839
H2 & H3	1.2427	1.2364	1.2275	1.2141

Note: Values below the perceptibility threshold (2.3) for CIELAB chromatic differences are presented in boldface.

close attention to changes in a patient’s facultative pigmentation due to tanning during that period. In the case of anemia, such changes are likely to render the monitoring of its distinct levels of severity impractical. As for the monitoring of distinct hyperbilirubinemia toxicity stages, the tanning-triggered masking effects are more likely to become a hindrance when transitions to extreme stages of this disorder are involved. For these situations, the use of optically-based approaches based on the analysis of spectral responses obtained in hypopigmented body areas [4], [6] are likely to lead to higher efficacy to cost ratios in both the screening and the monitoring of these medical conditions.

IV. CONCLUSION AND FUTURE WORK

In this paper, we have investigated the impact of tanning on the variations in skin chromatic attributes elicited by anemia and hyperbilirubinemia. Our findings, albeit still subject to *in vivo* confirmation, provide original insights about the distinct interactions between the visual symptoms of these conditions, and how they can be affected by tanning-induced changes in the cutaneous tissues’ melanin pigmentation and thickness. More explicitly, they indicate that these changes may have a stronger masking effect on skin paleness resulting from reductions in hemoglobin concentrations associated with anemia, than on skin yellowness resulting from increases in bilirubin concentrations associated with hyperbilirubinemia.

In our investigation, we have considered a skin specimen with a moderate tanning ability. For individuals with a stronger tanning ability, one would expect stronger masking effects. At a certain “turn-off” point, these effects may have an impact similar to that associated with high levels of constitutive pigmentation, and consequently render the visual differentiation between the distinct anemia severity levels and hyperbilirubinemia toxicity stages impractical.

Clearly, the precise magnitude of these effects varies from one individual to another, and its quantification under *in vivo*

TABLE VII: Row-wise CIELAB ΔE_{ab}^* values computed for the (tanned) specimen’s swatches depicted in Fig 5.

Hyperbilirubinemia Toxicity Stages	Anemia Severity Transitions		
	A0 & A1	A1 & A2	A2 & A3
H0	1.2739	1.1314	1.7449
H1	1.1385	2.1030	1.7358
H2	1.1694	2.1032	2.2464
H3	1.5921	1.1242	2.6211

Note: Values below the perceptibility threshold (2.3) for CIELAB chromatic differences are presented in boldface.

TABLE VIII: Column-wise CIELAB ΔE_{ab}^* values computed for the (tanned) specimen’s swatches depicted in Fig 5.

Hyperbilirubinemia Toxicity Transitions	Anemia Severity Levels			
	A0	A1	A2	A3
H0 & H1	7.8167	8.5305	9.9711	11.1466
H1 & H2	2.5341	2.7732	2.5116	2.8683
H2 & H3	1.0098	1.5076	0.8269	1.2464

Note: Values below the perceptibility threshold (2.3) for CIELAB chromatic differences are presented in boldface.

conditions would incur serious health risks. Alternatively, comprehensive databases, containing spectral responses, images and the specimens’ detailed characterization information, could be compiled using predictive *in silico* experimental frameworks. Such databases could then be used not only to estimate the aforementioned “turn-off” point, but also to support the development of new cost-effective protocols for the screening and monitoring of medical conditions associated with the onset of skin appearance changes. As future work, we intend to explore this research avenue.

The compilation of such *in silico* databases, however, would not diminish the importance of obtaining measured skin spectral data. Nowadays, a larger variety of optical devices are being proposed for assisting the prevention, diagnosis, monitoring and treatment of a wide range of diseases whose detection can be associated with the correct interpretation of variations in skin appearance attributes. Many of these devices employ computer algorithms/models that are used in the analysis of skin spectral responses to light stimulus in order, for example, to infer relevant biophysical parameters (*e.g.*, concentration and distribution of target substances within the cutaneous tissues) and to determine the dose and spatial distribution of radiation required for a given treatment. Besides their use in optical devices, computer models involving light transport in skin tissue are also extensively used to accelerate the generation and validation research hypotheses in several biomedical areas, and in the *in silico* testing of skin-protective products (*e.g.*, sunscreens).

The success of these applications depends on the correctness of the computer models used to support them. Hence, it is necessary to evaluate their predictive capabilities by comparing their outputs with measured spectral data, in particular skin reflectance, whose scarcity represents a critical obstacle in this context. The relatively few existing skin spectral datasets are usually limited to a handful of specimens whose reflectance data was measured considering only a single illumination/viewing geometry. Moreover, these

datasets include vague descriptions of the specimens. This makes the evaluation of models more prone to biases since the biophysical parameters used as input for a model may diverge considerably from the actual biophysical parameters associated with the specimen at hand. Hence, we believe that the biomedical community should continue to foster efforts aiming at increasing the availability of such fundamental datasets and making them more easily accessible.

REFERENCES

- [1] World Health Organization, "Haemoglobin concentrations for the diagnosis of anaemia and assessment of severity," in *VMNIS - Vitamin and Mineral Nutrition Information System*, Geneva, Switzerland, 2011, pp. 1–6, WHO/NMH/NHD/MnM/11.1.
- [2] J. Fevery, "Bilirubin in clinical practice: a review," *Liver International*, pp. 592–605, 2008.
- [3] US Department of Health and Human Services, "Your guide to anemia," Tech. Rep. NIH 11-7629, National Institutes of Health, National Heart, Lung and Blood Institute, September 2011.
- [4] G.V.G. Baranoski, A. Dey, and T.F. Chen, "Assessing the sensitivity of human skin hyperspectral responses to increasing anemia severity levels," *J. Biomed. Opt.*, vol. 9, no. 20, pp. 095002–1–14, 2015.
- [5] A. Maton, J. Hopkins, C. W. McLaughlin, S. Johnson, M. Q. Warner, D. LaHart, and J.D. Wright, *Human Biology and Health*, Prentice Hall, Englewood Cliffs, N.J., USA, 1993.
- [6] G.V.G. Baranoski, T.F. Chen, and P. Varsa, "On the effective differentiation and monitoring of variable degrees of hyperbilirubinemia severity through noninvasive screening protocols," in *40th Annual International Conference of the IEEE Engineering in Medicine and Biology Society (EMBC)*, Honolulu, HI, USA, July 2018, pp. 4981–4986.
- [7] S.D. Zucker, P.S. Horn, and K.E. Sherman, "Serum bilirubin levels in the US population: Gender effect and inverse correlation with colorectal cancer," *Hepatology*, vol. 40, no. 4, pp. 827–835, 2004.
- [8] F. Groenendaal, J. van der Grond, and L.S. de Vries, "Cerebral metabolism in severe neonatal hyperbilirubinemia," *Pediatrics*, vol. 114, no. 1, pp. 291–294, 2004.
- [9] R.P. Wennberg, C.E. Ahlfors, V.K. Bhutani, L.H. Johnson, and S.M. Shapiro, "Toward understanding kernicterus: A challenge to improve the management of jaundice newborns," *Pediatrics*, vol. 117, no. 2, pp. 474–485, 2006.
- [10] H. Özkan, H. Ören, N. Duman, and M. Duman, "Dermal bilirubin kinetics during phototherapy in term neonates," *Acta Paediatr.*, vol. 92, pp. 577–581, 2003.
- [11] C.J. Kapoor and C.R.K. Murti, "Role of human skin in the photodecomposition of bilirubin," *Biochem. J.*, vol. 142, pp. 567–573, 1974.
- [12] G.R. Buchanan and B.E. Glader, "Benign course of extreme hyperbilirubinemia in sickle cell anemia: Analysis of six cases," *The Journal of Pediatrics*, vol. 91, no. 1, pp. 21–24, 1977.
- [13] M.D. Hargrove, "Marked increase in serum bilirubin in sickle cell anemia a report of 6 patients," *Digest. Dis.*, vol. 15, no. 5, pp. 437–442, 1970.
- [14] S.A. Merrill, R.A. Brodsky, S.M. Lanzkron, and R. Naik, "A case-control analysis of hyperhemolysis syndrome in adults and laboratory correlates of complement involvement," *Transfusion*, vol. 59, pp. 3129–3139, 2019.
- [15] J. Phillips and A.C. Henderson, "Hemolytic anemia: Evaluation and differential diagnosis," *Am. Fam. Physician*, vol. 98, no. 6, pp. 354–361, 2018.
- [16] A. Rets, A.L. Clayton, R.D. Christensen, and A.M. Agarwal, "Molecular diagnostic update in hereditary hemolytic anemia and neonatal hyperbilirubinemia," *Int. J. Lab. Hematol.*, vol. 41, no. S1, pp. 95–101, 2019.
- [17] R. Carmnel, E.T. Wong, J.M. Weiner, and C.S. Johnson, "Racial differences in serum total bilirubin levels in health and in disease (pernicious anemia)," *JAMA*, vol. 253, no. 23, pp. 3416–3418, 1985.
- [18] R.E. Hannemann, D.P. Dewitt, E.J. Hanley, R.L. Schreiner, and P. Bonderman, "Determination of serum bilirubin by skin reflectance: Effect of pigmentation," *Pediatr. Res.*, vol. 13, pp. 1326–1329, 1979.
- [19] T.F. Chen and G.V.G. Baranoski, "A physiologically-based framework for the simulation of skin tanning dynamics," in *Proc. of SPIE, Vol. 10877, Dynamics and Fluctuations in Biomedical Photonics XVI: Tissue and Cell Dynamics, SPIE Photonics West - BiOS*, M.J. Leahy V.V. Tuchin and R.W. Wang, Eds., San Francisco, CA, USA, March 2019, pp. 108770H–1–20, Supplemental video: <https://www.youtube.com/watch?v=I1quYM34wWw>.
- [20] G.V.G. Baranoski, P. Alencar, Spencer R. Van Leeuwen, and Tenn F. Chen, "Tanning-elicited variations in the ultraviolet absorption spectra of the cutaneous tissues: Skin photobiology and photomedicine implications," in *43rd Annual International Conference of the IEEE Engineering in Medicine and Biology Society (EMBC)*, Virtual Conference, October 31 - November 4 2021, pp. 4268–4273.
- [21] M. Viceconti, A. Henney, and E. Morley-Fletcher, "In silico clinical trials: How computer simulation will transform the biomedical industry," *Int. J. Clin. Trials*, vol. 3, no. 2, pp. 37–46, 2016.
- [22] S.A. Prahl, "Optical absorption of hemoglobin," Tech. Rep., Oregon Medical Laser Center, 1999.
- [23] S.A. Prahl, "PhotochemCAD spectra by category," Tech. Rep., Oregon Medical Laser Center, 2001.
- [24] H. Du, R.A. Fuh, J. Li, A. Corkan, and J.S. Lindsey, "PhotochemCAD: A computer aided design and research tool in photochemistry," *Photochemistry and Photobiology*, vol. 68, no. 2, pp. 142–142, 1998.
- [25] S.L. Jacques, "Optical absorption of melanin," Tech. Rep., Oregon Medical Laser Center, 2001.
- [26] T.F. Chen, G.V.G. Baranoski, B.W. Kimmel, and E. Miranda, "Hyperspectral modeling of skin appearance," *ACM Trans. Graph.*, vol. 34, no. 3, pp. 31:1–14, 2015, Supplemental video: <https://www.youtube.com/watch?v=hKvIWS5H94s>.
- [27] G.V.G. Baranoski, S.R. van Leeuwen, and T.F. Chen, "On the detection of peripheral cyanosis in individuals with distinct levels of cutaneous pigmentation," in *39th Annual International Conference of the IEEE Engineering in Medicine and Biology Society (EMBC)*, Jeju Island, South Korea, August 2017, pp. 4260–4264.
- [28] A. T. Lovell, J. C. Hebden, J. C. Goldstone, and M. Cope, "Determination of the transport scattering coefficient of red blood cells," in *Proc. SPIE 3597, Optical Tomography and Spectroscopy of Tissue III*, 1999, vol. 3597, pp. 175–182.
- [29] R. Flewelling, "Noninvasive optical monitoring," in *The Biomedical Engineering Handbook*, Joseph D. Bronzino, Ed. CRC Press LLC, 2 edition, 2000.
- [30] V.K. Bhutani, G.R. Gourley, S. Adler, B. Kreamer, C. Dalin, and L.H. Johnson, "Noninvasive measurement of total serum bilirubin in a multiracial predischarge newborn population to assess the risk of severe hyperbilirubinemia," *Pediatrics*, vol. 106, no. 2, pp. 1–9, 2000.
- [31] K.M. Van de Graaff, *Human Anatomy*, W. C. Brown Publishers, Dubuque, IO, USA, 4th edition, 1995.
- [32] S. Askew and G.V.G. Baranoski, "On the dysfunctional hemoglobins and cyanosis connection: Practical implications for the clinical detection and differentiation of methemoglobinemia and sulfhemoglobine-mia," *Biomed. Opt. Express*, vol. 9, no. 1, pp. 3284–3305, 2018.
- [33] S.R. van Leeuwen and G.V.G. Baranoski, "Elucidating the contribution of Rayleigh scattering to the bluish appearance of veins," *J. Biomed. Opt.*, vol. 23, no. 2, pp. 025001–1–17, 2018.
- [34] G.V.G. Baranoski, J.G. Rokne, and G. Xu, "Virtual spectrophotometric measurements for biologically and physically-based rendering," *The Visual Computer*, vol. 17, no. 8, pp. 506–518, 2001.
- [35] G.V.G. Baranoski, T. Dimson, T.F. Chen, B. Kimmel, D. Yim, and E. Miranda, "Rapid dissemination of light transport models on the web," *IEEE Comput. Graph.*, vol. 32, pp. 10–15, 2012.
- [36] Natural Phenomena Simulation Group (NPSG), *Run HyLloS Online*, School of Computer Science, University of Waterloo, Ontario, Canada, 2017, <http://www.npsg.uwaterloo.ca/models/hyliosEx.php>.
- [37] Natural Phenomena Simulation Group (NPSG), *Human Skin Data*, School of Computer Science, University of Waterloo, Ontario, Canada, 2014, <http://www.npsg.uwaterloo.ca/data/skin.php>.
- [38] R.W.G. Hunt, *Measuring Colour*, Ellis Horwood Limited, Chichester, England, 2nd edition, 1991.
- [39] G.V.G. Baranoski and A. Krishnaswamy, *Light & Skin Interactions: Simulations for Computer Graphics Applications*, Morgan Kaufmann/Elsevier, Burlington, MA, USA, 2010.
- [40] M. Stokes, M.D. Fairchild, and R.S. Berns, "Precision requirements for digital color reproduction," *ACM Trans. Graph.*, vol. 11, no. 4, pp. 406–422, 1992.
- [41] D.H. Brainard, "Color appearance and color difference specification," *The Science of Color*, vol. 2, pp. 191–216, 2003.
- [42] M. Mahy, L. Van Eycken, and A. Oosterlinck, "Evaluation of uniform color spaces developed after the adoption of CIELAB and CIELUV," *Color Research and Application*, vol. 19, no. 2, pp. 105–121, 1994.